The Carnitine Shuttle Pathway is Altered in Patients With Neovascular Age-Related Macular Degeneration

Sabrina L. Mitchell,[1] Karan Uppal,[2] Samantha M. Williamson,[1] Ken Liu,[2] L. Goodwin Burgess,[1] ViLinh Tran,[2] Allison C. Umfress,[1] Kelli L. Jarrell,[1] Jessica N. Cooke Bailey,[3] Anita Agarwal,[1] Margaret Pericak-Vance,[4] Jonathan L. Haines,[3] William K. Scott,[4] Dean P. Jones,[2] and Milam A. Brantley Jr[1]

[1]Vanderbilt Eye Institute, Vanderbilt University Medical Center, Nashville, Tennessee, United States
[2]Department of Medicine, Emory University Medical Center, Atlanta, Georgia, United States
[3]Department of Population and Quantitative Health Sciences, Institute for Computational Biology, Case Western Reserve University, Cleveland, Ohio, United States
[4]John P. Hussman Institute for Human Genomics, University of Miami Miller School of Medicine, Miami, Florida, United States

Purpose. To identify metabolites and metabolic pathways altered in neovascular age-related macular degeneration (NVAMD).

Methods. We performed metabolomics analysis using high-resolution C18 liquid chromatography-mass spectrometry on plasma samples from 100 NVAMD patients and 192 controls. Data for mass/charge ratio ranging from 85 to 850 were captured, and metabolic features were extracted using xMSanalyzer. Nested feature selection was used to identify metabolites that discriminated between NVAMD patients and controls. Pathway analysis was performed with Mummichog 2.0. Hierarchical clustering was used to examine the relationship between the discriminating metabolites and NVAMD patients and controls.

Results. Of the 10,917 metabolic features analyzed, a set of 159 was identified that distinguished NVAMD patients from controls (area under the curve of 0.83). Of these features, 39 were annotated with confidence and included multiple carnitine metabolites. Pathway analysis revealed that the carnitine shuttle pathway was significantly altered in NVAMD patients ($P = 0.0001$). Tandem mass spectrometry confirmed the molecular identity of five carnitine shuttle pathway acylcarnitine intermediates that were increased in NVAMD patients. Hierarchical cluster analysis revealed that 51% of the NVAMD patients had similar metabolic profiles, whereas the remaining 49% displayed greater variability in their metabolic profiles.

Conclusions. Multiple long-chain acylcarnitines that are part of the carnitine shuttle pathway were significantly increased in NVAMD patients compared to controls, suggesting that fatty acid metabolism may be involved in NVAMD pathophysiology. Cluster analysis suggested that clinically indistinguishable NVAMD patients can be separated into distinct subgroups based on metabolic profiles.

Keywords: metabolomics, age-related macular degeneration, long-chain acylcarnitines, carnitine shuttle

A ge-related macular degeneration (AMD) is the leading cause of blindness in developed countries and is responsible for 8.7% of all blindness worldwide.[1] Neovascular AMD (NVAMD), in which blood or serous fluid leaks from abnormal choroidal or retinal vessels, is responsible for the majority of cases of AMD-related vision loss.[2] The annual incidence of NVAMD in the United States has been calculated at 1.8%, resulting in an estimated 160,000 new cases each year.[3]

The etiology of NVAMD is complex, comprising genetic and environmental factors. More than 30 genetic loci have been associated with AMD risk.[4] Additional risk factors include advanced age, smoking, and body mass index (BMI).[5,6] While there have been significant advances in NVAMD treatment, a more detailed understanding of AMD pathophysiology could facilitate development of new NVAMD prevention and therapeutic strategies.

Metabolomics is one approach to discerning more comprehensively the molecular pathophysiology of disease. High-resolution metabolomics detects endogenous and exogenous metabolites in biofluids. The goal of metabolomics analysis is to identify specific metabolites and metabolic pathways that are altered in different health states. This approach has been increasingly applied to ophthalmologic conditions,[7] and several metabolomics studies have identified metabolites with altered plasma levels in AMD patients compared to controls.[8–11] We previously used high-resolution liquid chromatography with mass spectrometry (LC-MS) to perform the first metabolome-wide association study of AMD, comparing NVAMD patients to

4978

controls. While this original AMD metabolomics study had a relatively small sample size, we identified differences between NVAMD patients and controls in individual metabolites including amino acids, vitamin D-related metabolites, and bile acids.[8]

For the current investigation, we performed high-resolution metabolomics via LC-MS in an entirely new and larger cohort of NVAMD patients ($n = 100$) and controls ($n = 192$) to determine individual metabolites and metabolic pathways altered in NVAMD. Using a combination of statistical and machine learning methods, we identified metabolic features altered in NVAMD patients, and evaluated their ability to accurately discriminate between NVAMD patients and controls. Additionally, these metabolic features were used to identify biological pathways that may be altered in NVAMD.

METHODS

Ethics Statement

This study was approved by the Vanderbilt University Medical Center Human Research Protection Program. Research adhered to the tenets of the Declaration of Helsinki and was conducted in accordance with Health Insurance Portability and Accountability Act regulations. Written informed consent was obtained from all participants before study enrollment.

Study Participants

Study participants were recruited from the Vanderbilt Eye Institute between 2002 and 2011. All patients were of European descent and at least 55 years old at enrollment. Each participant underwent a comprehensive eye exam administered by a fellowship-trained retina specialist that included slit-lamp biomicroscopy and dilated fundus examination with indirect ophthalmoscopy. High-resolution color fundus photography was obtained via a Zeiss 450+ fundus camera (Carl Zeiss Meditec, Dublin, CA, USA). Using the five-step Clinical Age-Related Maculopathy Scale (CARMS),[12] a modified version of the Age-Related Eye Disease Study (AREDS) grading system,[13] each participant was assigned an AMD grade from 1 to 5 based on the more severely affected eye. For the current study, cases were NVAMD patients ($n = 100$) with AMD Grade 5 in one or both eyes. Grade 5 was defined as extensive AMD characterized by choroidal neovascularization, subretinal hemorrhage or fibrosis, or photocoagulation scarring consistent with AMD treatment. Of the 100 NVAMD patients, 92 had Grade 5 in both eyes, while the remaining eight had Grade 4 (geographic atrophy) in the fellow eye. Controls ($n = 192$) were patients with AMD Grade 1 in both eyes, defined as fewer than 10 small drusen and no macular pigment changes.

At study enrollment, using a 21- or 23-gauge butterfly needle, blood was drawn from participants into 8.5 mL Acetate-Citrate-Dextrose tubes containing 1.5 mL Solution A (trisodium citrate 22.0 g/L, citric acid 8.0 g/L, and dextrose 24.5 g/L; Becton Dickinson, Franklin Lakes, NJ, USA). These tubes were centrifuged for 10 minutes at 4°C. Plasma was transferred to 1.5 mL conical tubes and immediately stored at −80°C.

Detailed demographic information and history of environmental exposures and comorbid medical conditions, including height and weight, smoking status, diabetes, hypertension, and hyperlipidemia, were collected via a self-administered questionnaire. BMI was calculated using the reported height and weight. Participants who indicated they had ever smoked at least 100 cigarettes were considered smokers, while those who had smoked fewer than 100 cigarettes were considered nonsmokers.

High-Resolution Untargeted Metabolomics

Frozen plasma samples were thawed and analyzed by LC-MS at Emory University as described previously.[14–19] Plasma samples were randomized into 20-sample batches that included NVAMD patients and controls. Plasma aliquots (65 μL) were treated with 130 μL acetonitrile (2:1 vol/vol) containing 3.5 μL of an internal isotopic standard mix[17–19] and placed on ice for 30 minutes. Samples then were centrifuged for 10 minutes (16,100g at 4°C) to remove protein. The supernatants (10 μL) were loaded onto an Accela Open Autosampler maintained at 4°C. Each sample was analyzed in triplicate using a Thermo LTQ Velos Orbitrap high-resolution (60,000 mass resolution) mass spectrometer (Thermo Fisher Scientific, San Diego, CA, USA) and C18 column chromotography.[14,20] Elution was obtained with a formic acid/acetonitrile gradient at a flow rate of 0.35 mL/min for the initial 6 minutes and 0.5 mL/min for the remaining 4 minutes. The first 2-minute period consisted of 5% solution A (2% [vol/vol] formic acid in water), 60% water, 35% acetonitrile. The final 4-minute period was maintained at 5% solution A, 95% acetonitrile. The mass spectrometer was set to collect mass/charge ratio (m/z) ranging from 85 to 850 over 10 minutes. Electrospray ionization was used in positive mode for detection. For quality control and assurance, pooled reference plasma was run before and after each batch of samples.

Data Processing and Analysis

An adaptive processing software package, apLCMS (available in the public domain at http://web1.sph.emory.edu/apLCMS/), designed for use with high-resolution mass spectrometry data, was used for noise removal and feature extraction, alignment, and quantification.[21] Each metabolic feature is defined by a unique combination of m/z and retention time (RT). To enhance the feature detection process and perform quality evaluation, systematic data re-extraction and statistical filtering were performed using xMSanalyzer (available in the public domain at http://sourceforge.net/projects/xmsanalyzer/).[22] Each sample was analyzed in triplicate, and coefficient of variation (CV) was used to evaluate the quality of all features. Pearson correlation within technical replicates was used to evaluate the quality of samples.

Batch-effect correction was performed using ComBat.[23] A $\log_2$ transformation was applied to reduce heteroscedasticity and normalize results. Quantile normalization was performed to reduce between-sample variability.[24] To increase confidence for selection of discriminating metabolites, data were filtered based on missing value criteria and only those features present in at least 80% of either cases or controls and present in at least 50% of all samples were included in downstream statistical analyses.

Feature Selection and Annotation

As is common practice when using machine learning methods, the cases and controls were randomly divided into training and test sets containing 70% and 30% of samples, respectively.[25] The training set included 70 NVAMD patients and 134 controls, while the test set included 30 NVAMD patients and 58 controls. Nested feature selection was performed on the training set using linear models for microarray data (LIMMA), variable importance for projection (VIP) based on partial least squares discriminant analysis (PLS-DA), support vector machine recursive feature elimination (SVM-RFE), and random forest, incorporated in the R packages CMA and mixOmics.[26] Using the *GenerateLearningsets* function in the CMA package, the training set was randomly split into learning sets and validation

sets 100 times, such that, for each iteration, the proportion of cases and controls was the same as for the whole data set. The *GeneSelection* function in the CMA package was used to perform feature selection in each learning set.[26] To allow for identification of the most robust features and reduce the risk of selecting noisy features, the final set of discriminating features included those selected in at least 70% of learning sets by one or more of the feature selection methods.[27]

Following nested feature selection, the fold change between NVAMD patients and controls was calculated for each discriminating feature. The features were annotated using the R package xMSannotator, which uses a multilevel clustering procedure based on intensity across all samples, retention time, mass defect, and isotope/adduct patterns.[28] Additionally, xMSannotator uses metabolic pathway associations to assign confidence levels for database matches. Confidence levels range from zero to three, designating annotations from no to high confidence, which reduces the risk of false annotations and allows prioritization of computationally derived annotations for further experimental evaluation and confirmation.[28]

Pathway Analysis and Hierarchical Cluster Analysis

The discriminating features were used to perform pathway analysis via Mummichog 2.0 (available in the public domain at http://mummichog.org/), a program that combines metabolite identification and metabolic pathway/network analysis.[29,30] Pathways with an overlap size of four or greater were evaluated further by ion dissociation mass spectrometry. Using the *hclust()* function in R, 2-way hierarchical cluster analysis was performed to visualize the relationship between discriminating metabolite values and case-control status.

Ion Dissociation Mass Spectrometry (LC-MS/MS)

Ion dissociation mass spectrometry was performed for representative discriminating metabolites detected in the study samples. Samples were analyzed using a Thermo LTQ Velos Orbitrap high-resolution (60,000 mass resolution) mass spectrometer (Thermo Fisher Scientific, San Diego, CA, USA) operated in positive ion mode with 10-minute C18 column chromatography and standard source conditions used for the untargeted metabolic profiling. Before analysis, plasma proteins were precipitated using acetonitrile (2:1 vol/vol) and allowed to equilibrate for 30 minutes. Collision-induced ion dissociation was accomplished using high purity N_2 at a normalized collision energy of 35%. The tandem mass spectrometry data were processed using the *xcmsFragments* function in XCMS,[31–33] and the experimental spectra were compared with in-silico fragmentation using MetFrag.[34]

Classification Accuracy Evaluation

The *classification()* function in the R package CMA was used to test the classification performance of the discriminating features using the support vector machine (SVM) classifier.[26] Using the training set, the SVM hyperparameters were selected by applying the *tune()* function in the CMA package. The *evaluation()* function was used to assess the classification accuracy based on the mean accuracy across the validation sets and the overall accuracy in the test set, using area under the receiver operating characteristic curve (AUROC) criteria. Additionally, balanced accuracy rate (BAR) was calculated, where $BAR = (C_{NVAMD} + C_{control})/2$, C_{NVAMD} is the number of correctly classified subjects in the NVAMD group, and $C_{control}$ is

TABLE 1. Study Population Characteristics

Characteristic	Controls ($n = 192$)	NVAMD ($n = 100$)	P Value
Age, y	71.9	79.2	4.8×10^{-16}
Female, %	64.0	65.0	0.976
Smokers, %	49.5	61.0	0.080
BMI, kg/m²	26.9	26.8	0.801
Diabetes, %	18.0	23.3	0.401
Hypertension, %	51.4	60.9	0.180
Hyperlipidemia, %	53.7	49.4	0.604

Demographic, environmental, and clinical characteristics were compared between NVAMD patients and controls using a *t*-test for continuous variables and a χ^2 test for categorical variables. The mean age and mean BMI are presented.

the number of correctly classified subjects in the control group.

Statistical Analysis

Descriptive statistics for demographic and clinical variables were calculated for the entire study population. Comparisons between NVAMD patients and controls were made using a 2-tailed *t*-test for continuous data (age and BMI) and a χ^2 test for categorical data (sex, smoking status, diabetes, hypertension, and hyperlipidemia). Using these same tests, we compared demographic, environmental, and clinical variables between the NVAMD patients from Cluster 1 and NVAMD patients from all other clusters identified in the hierarchical cluster analysis to determine if these variables differed between these two groups.

To test for association between discriminating features and age and sex, we performed separate linear regressions for each feature, including age and sex in the regression model. A Bonferroni correction for multiple testing was performed to obtain an adjusted significance threshold.

RESULTS

The study population consisted of 292 patients, including 100 NVAMD patients and 192 controls. Demographic variables, environmental exposures, and comorbid medical conditions were compared between NVAMD patients and controls (Table 1). While NVAMD patients were older than controls, there were no significant associations between NVAMD and sex, BMI, smoking status, diabetes, hypertension, or hyperlipidemia in this population.

Mass spectral data from LC-MS analysis of the 292 samples yielded 18,881 ions (defined by *m/z* and RT), each with an associated ion intensity. After data preprocessing and filtering based on missing values, 10,917 features were used for further analyses. The study population was divided into training and test sets. The training set was used to identify potential discriminating metabolites, and the test set was used to assess the generalizability of the results and determine how well those metabolites are able to differentiate between NVAMD patients and controls in an independent set of samples. Nested feature selection was performed on the training set with the 10,917 features, and a group of 159 metabolic features that discriminate NVAMD patients from controls was identified (Supplemental Table S1). Of these discriminating features, 110 were increased and 49 were decreased in the plasma of NVAMD patients compared to controls.

Age and sex can be associated with metabolite levels.[35] To determine if these factors affected plasma levels of the

discriminating features in this study, separate linear regressions were performed for each of the 159 metabolites, including age and sex as covariates. After correction for multiple testing, neither age nor sex was associated with levels of any of these metabolites (Supplementary Table S1).

The 159 discriminating features were annotated using xMSannotator. Of these metabolites, 39 were annotated with medium or high confidence (Table 2). Among these, multiple features were annotated to acylcarnitines, bile acids, phospholipids, lysophospholipids, and amino acids. To investigate further, we performed pathway analysis with Mummichog 2.0. This analysis showed that carnitine shuttle pathway metabolites ($P = 0.0001$; overlap size, 6 of 27) and bile acid biosynthesis pathway metabolites ($P = 0.013$; overlap size, 3 of 22) were overrepresented among the 159 discriminating features. After adjusting for multiple comparisons using Bonferroni correction, the carnitine shuttle pathway remained significant, suggesting that this pathway is altered in NVAMD patients.

Given that pathway analysis identified the carnitine shuttle, and that multiple discriminating features were putatively annotated to carnitines by xMSannotator, we performed LC-MS/MS to confirm the molecular identity of the six metabolites associated with the carnitine shuttle pathway. LC-MS/MS analysis supported the identity of five of these features as acylcarnitine intermediates (Table 3). As measured in the untargeted LC-MS, plasma levels of these long-chain acylcarnitines were significantly increased between 1.7 and 2.2-fold in NVAMD patients compared to controls (Table 3; Fig. 1).

Hierarchical clustering was performed using the training set to visualize how well the 159 discriminating features differentiate NVAMD patients from controls. The results demonstrated separation of the 204 individuals of the training set into 11 clusters (Fig. 2). Of the 70 NVAMD patients, 36 (51.4%) clustered tightly together in Cluster 1, which also included eight controls, indicating that these patients share a similar metabolic profile in the context of the 159 discriminating features. In contrast, the remaining 34 NVAMD patients were distributed across five other clusters, each including a mixture of cases and controls. The remaining five clusters included only controls. To ensure that the clustering of the NVAMD patients was not due to differences in demographic or clinical variables, we compared these variables between NVAMD patients from Cluster 1 and the NVAMD patients from all other clusters. The tightly clustered NVAMD patients from Cluster 1 and the remaining NVAMD patients did not differ by any demographic, environmental, or clinical variables (Supplementary Table S2), indicating that the clustering of NVAMD patients is not due to any of these variables.

We evaluated the ability of the 159 metabolic features identified using the training set to accurately discriminate NVAMD patients and controls in the test set. Using the SVM classifier, the 159 features produced a 10-fold cross-validation balanced accuracy rate of 96.1% in the training set and a balanced accuracy rate of 75.6% along with an area under the curve (AUC) of 0.83 in the test set.

DISCUSSION

This large metabolome-wide association study identified a set of 159 metabolites that partially discriminated between NVAMD patients and controls in our cohort. Annotation of the discriminating features using computational methods followed by LC-MS/MS demonstrated differences in levels of multiple long-chain acylcarnitines. Further evaluation of the features using pathway analysis revealed that the carnitine

shuttle pathway was significantly altered in NVAMD patients. Additionally, hierarchical cluster analysis revealed the potential for clinically indistinguishable NVAMD patients to be classified into metabolically distinct subgroups based on levels of discriminating features.

Evidence suggests that lipid metabolism is a key factor in the pathogenesis of AMD. Genes involved in lipid and lipoprotein metabolism pathways have been associated with AMD,[4,36] and previous AMD metabolomics studies have pointed to altered lipid metabolism.[9,10] In our study, multiple long-chain acylcarnitines from the carnitine shuttle pathway were increased in NVAMD patients compared to controls. Among these long-chain acylcarnitines was L-palmitoylcarnitine which was reported to be altered in a small cohort of Chinese NVAMD patients compared to a non-AMD control group.[11] The carnitine shuttle pathway is responsible for transporting long-chain fatty acids into the mitochondria for subsequent catabolism via β-oxidation, in a process that requires acyl-CoA and results in the esterification of L-carnitine to form acylcarnitine derivatives.[37] Additionally, in a gene-based pathway analysis comparing exome sequence results in NVAMD patients to non-AMD controls, Sardell et al.[38] identified enrichment of variants in the biosynthesis of unsaturated fatty acids pathways. Thus, multiple lines of evidence suggest that fatty acid metabolism may be involved in NVAMD pathogenesis.

Increased plasma levels of long-chain acylcarnitines have been reported in other conditions, including cardiovascular disease,[39] heart failure,[40] and type 2 diabetes.[41] Each condition has risk factors that also have been associated with AMD (e.g., hypertension, hyperlipidemia) suggesting common mechanisms could be contributing to these diseases. It is possible that perturbation of the carnitine shuttle leads to compromised mitochondrial function, which could decrease cellular capacity to handle reactive oxygen species, resulting in increased cellular dysfunction and cell death. Targeted investigations of carnitine shuttle enzymes and metabolites are necessary to determine how the alterations in long-chain acylcarnitines might contribute to NVAMD pathogenesis.

We also observed that some metabolic features with matches to taurine-conjugated bile acids were increased in NVAMD patients compared to controls. The bile acid biosynthesis pathway was identified in the pathway analysis, but was not significant after correction for multiple testing. In our previous AMD metabolomics study, we identified the bile acid biosynthesis pathway as altered in NVAMD patients.[8] The features identified in that study were matched to glycine-conjugated bile acids and were decreased in NVAMD patients. Taken together, the data from these two studies suggest that bile acids are altered in NVAMD. Additional validation studies are necessary to confirm these findings, and molecular investigations are essential to determine the role of bile acids in disease pathogenesis.

The hierarchical cluster analysis revealed distinct metabolic profiles among NVAMD patients. Just over half of the NVAMD patients in the training set exhibited similar metabolic profiles and were assigned to a single cluster that included only eight control samples. No clear metabolic relationship was identified among the remaining NVAMD patients. We detected no differences in demographic characteristics or comorbidities between the NVAMD patients from the single cluster and the remaining NVAMD patients, suggesting the observed clustering is due to differences in plasma metabolic profiles. This metabolic heterogeneity likely contributed to the modest classification accuracy achieved when evaluating the 159 metabolites for their ability to accurately classify NVAMD patients and controls in the test set. Given the tight clustering of the NVAMD patients in Cluster 1, we hypothesize that these

TABLE 2. Discriminating Features Annotated With Confidence

_m/z_	Retention Time (Seconds)	Fold Change	Putative Match (Chemical ID)
347.2217	217.7	5.90	Pinusolide (HMDB35130), (-)-Chimonanthine (HMDB30280), 10-Dehydrogingerdione (HMDB29476), 4-Deoxyhumulone (HMDB36624), 12-Hydroxy-11-methoxy-81113-abietatrien-20-oic acid (HMDB38031), 4-Deoxyadhumulone (HMDB37378), Corticosterone (HMDB01547), 21-Deoxycortisol (HMDB04030), ()-Calycanthine (HMDB29561), 19-Hydroxydeoxycorticosterone (HMDB12612), 21-Hydroxy-5b-pregnane-31120-trione (HMDB06756), 7-Carboxy-alpha-tocotrienol (HMDB12849), Cortexolone (HMDB00015)
220.0573	305.3	5.24	L-Oxalylalbizziine (HMDB39164)
251.1494	315.4	3.55	Isopentyl beta-D-glucoside (HMDB34750)
163.0545	222.9	3.16	1-Tridecene-357911-pentayne (HMDB35400), Methomyl (HMDB31804)
508.3758	359.3	2.45	LysoPC(P-18:0) (HMDB13122)
427.3570	360.3	2.23	29-Norcycloartane-324-dione (HMDB32084), 4alpha-Formyl-4beta-methyl-5alpha-cholesta-824-dien-3beta-ol (HMDB12167), Stigmast-22-ene-36-dione (HMDB31931), Stigmast-4-ene-36-dione (HMDB38063), (6beta22E)-6-Hydroxystigmasta-422-dien-3-one (HMDB39425), 7-Oxostigmasterol (HMDB30015), Momordenol (HMDB31080), (3beta23E)-3-Hydroxy-27-norcycloart-23-en-25-one (HMDB37382)
425.3447	333.3	2.20	(22E24R)-Stigmasta-422-diene-36-dione (HMDB38656), Alpha-Tocotrienol (HMDB06327)
398.3261	352.8	2.17	9-Hexadecenoylcarnitine (HMDB13207), trans-Hexadec-2-enoyl carnitine (HMDB06317)
414.3575	343.4	2.16	Heptadecanoyl carnitine (HMDB06210)
274.1276	400.7	2.10	N-Despropyl-rotigotine (HMDB60841), Glutaconylcarnitine (HMDB13129)
401.3434	322.9	2.06	7-Ketocholesterol (HMDB00501), 7a-Hydroxy-cholestene-3-one (HMDB01993), Cholesta-814-diene-36-diol (HMDB34328), Calcidiol (HMDB03550), 56-trans-25-Hydroxyvitamin D3 (HMDB06721), 25-Hydroxytachysterol3 (HMDB06722), Alfacalcidol (HMDB15504), (3beta5alpha6a)-1-Phenyl-13-heneicosanedione (HMDB35585), 5-Methyl-24-bis(3-methyl-2-butenyl)-6-(2-methyl-1-oxopropyl)-5-(4-methyl-3-pentenyl)cyclohexanone (HMDB36012), 5-(1215-Heneicosadienyl)-13-benzenediol (HMDB39871), 3beta-Hydroxy-5-cholestenal (HMDB60131), 27alpha-Hydroxy-8-dehydrocholesterol (HMDB60132)
426.3566	342.8	2.03	Oleoylcarnitine (HMDB05065), 11Z-Octadecenylcarnitine (HMDB13338), Vaccenyl carnitine (HMDB06351), Elaidic carnitine (HMDB06464)
400.3386	304.6	1.95	L-Palmitoylcarnitine (HMDB00222)
548.2445	325.0	1.88	Darunavir (HMDB15393)
506.3576	510.2	1.78	LysoPC(P-18:1(9Z)) (HMDB10408)
367.2715	427.1	1.74	Bepridil (HMDB15374)
396.3106	274.1	1.72	912-Hexadecadienoylcarnitine (HMDB13334)
491.1502	313.4	1.69	456-Trimethylscutellarein 7-glucoside (HMDB40512)
428.3709	376.7	1.65	Stearoylcarnitine (HMDB00848)
130.0499	196.7	1.64	1-Pyrroline-4-hydroxy-2-carboxylate (HMDB02234), Pyroglutamic acid (HMDB00267), Pyrroline hydroxycarboxylic acid (HMDB01369), N-Acryloylglycine (HMDB01843), 5-Oxoprolinate (HMDB60262), Pyrrolidonecarboxylic acid (HMDB00805), Dimethadione (HMDB61093)
274.6253	332.9	1.61	Darunavir (HMDB15393)
511.3602	379.5	1.53	LysoPC(17:0) (HMDB12108), LysoPE(0:020:0) (HMDB11481), LysoPE(20:00:0) (HMDB11511)
508.3390	387.7	1.52	Gymnodimine (HMDB41430), LysoPE(20:1(11Z)0:0) (HMDB11512), LysoPE(0:020:1(11Z)) (HMDB11482)
275.1255	321.0	1.50	Rutacultin (HMDB34132), 3-(11-Dimethyl-2-propenyl)-78-dimethoxy-2H-1-benzopyran-2-one (HMDB33921)Gossyvertin (HMDB39660), Batatasin II (HMDB40929)
494.3240	311.8	1.49	LysoPC(16:1(9Z)) (HMDB10383)
258.1097	307.2	1.39	Pyro-L-glutaminyl-L-glutamine (HMDB39229), 5-Methylcytidine (HMDB00982), Glycerophosphocholine (HMDB00086)
457.2333	248.4	1.32	1-Lyso-2-arachidonoyl-phosphatidate (HMDB12496)
479.3323	493.6	1.29	Dolicholide (HMDB34086), Polyporusterone A (HMDB38495)
493.1446	363.9	1.29	Americanin B (HMDB37338)
517.3065	331.6	1.25	Taurallocholic acid (HMDB00922), Taurocholic acid (HMDB00036), Tauro-b-muricholic acid (HMDB00932), Tauroursocholic acid (HMDB00889), Taurohyocholate (HMDB11637), LysoPC(18:4(6Z9Z12Z15Z)) (HMDB10389)
535.2946	252.2	1.22	Corchoroside A (HMDB33846)
516.3040	331.2	1.21	Taurallocholic acid (HMDB00922), Tauro-b-muricholic acid (HMDB00932), Tauroursocholic acid (HMDB00889), Taurocholic acid (HMDB00036), Taurohyocholate (HMDB11637), LysoPC(18:4(6Z9Z12Z15Z)) (HMDB10389)
240.0997	253.0	1.21	N-Ornithyl-L-taurine (HMDB33519)
649.3840	282.8	0.90	Lyciumoside III (HMDB39553)
818.5702	523.9	0.85	Multiple matches to phosphatidylethanolamine species
395.2762	395.4	0.59	2-(1415-Epoxyeicosatrienoyl) Glycerol (HMDB13651), 11-Hydroxyeicosatetraenoate glyceryl ester (HMDB12530)
318.3001	253.8	0.47	Phytosphingosine (HMDB04610)
247.1438	162.7	0.39	Lenticin (HMDB61115)
241.1055	192.4	0.29	Ethyl 345-trimethoxybenzoate (HMDB38627), 3-Carboxy-4-methyl-5-propyl-2-furanpropionic acid (HMDB61112), Isopropyl 3-(34-dihydroxyphenyl)-2-hydroxypropanoate (HMDB41756), 3-(345-Trimethoxyphenyl)propanoic acid (HMDB30254)

Of the 159 discriminating features, 39 were annotated by xMSannotator with medium or high confidence. _m/z_ = mass-to-charge ratio. Fold change was calculated as NVAMD patients versus controls.

TABLE 3. Features of the Carnitine Shuttle Pathway Verified by LC-MS/MS

m/z	Retention Time (Seconds)	Metabolite	Fold Change	P Value
398.3261	352.8	9-Hexadecenoylcarnitine (HMDB13207)	2.17	3.63×10^{-08}
414.3575	343.4	Heptadecanoyl carnitine (HMDB06210)	2.16	5.60×10^{-08}
426.3566	342.8	11Z-Octadecenylcarnitine (HMDB13338)	2.03	2.64×10^{-09}
400.3386	304.6	L-Palmitoylcarnitine (HMDB00222)	1.95	2.94×10^{-08}
428.3709	376.7	Stearoylcarnitine (HMDB00848)	1.65	2.37×10^{-08}

LC-MS/MS was used to confirm the identities of the carnitine shuttle pathway long-chain acylcarnitines (metabolite identification confidence level 2[42,43]). Fold change was calculated in the training set as NVAMD patients versus controls. Metabolite values were compared between NVAMD patients and controls using a *t*-test.

patients represent a metabolically-defined subgroup of NVAMD patients that could be of clinical importance. It is possible that metabolic variation could be responsible for some differences observed among AMD patients in the timing of disease progression. Further investigations in larger cohorts may allow for subcategorization of AMD patients based on metabolic profiles that could lead to improvements in clinical surveillance or treatment.

The large cohort of nearly 300 NVAMD patients and controls ascertained from the same institution with consistent sample collection and processing is a strength of this study. However, the study does not include intermediate AMD patients. Therefore, it cannot be determined if the differences observed between the groups are related specifically to NVAMD or to AMD in general. Additionally, given the complexity of determining the precise treatment history relative to the plasma sample collection date, AMD treatment was not considered in the analysis. An additional strength of this study was the use of high-resolution LC-MS in combination with powerful analytical tools. Untargeted high-resolution LC-MS is a sensitive technique that provides broad coverage of low and high abundance endogenous, environmental, and dietary metabolites. This increases the likelihood of identifying metabolites that are potentially relevant to AMD pathophysiology. However, untargeted metabolomics via LC-MS provides limited information on structural identity, and additional studies using tandem mass spectrometry are necessary to verify metabolite identities. In this study, to enhance confidence in metabolite annotations, we prioritized features from significant pathways and used a combination of computational methods and targeted tandem mass spectrometry.

In summary, this metabolomics study identified multiple long-chain acylcarnitines elevated in the plasma of NVAMD patients, suggesting that alterations in the carnitine shuttle pathway contribute to NVAMD pathophysiology. Further investigation is necessary to determine if the elevated
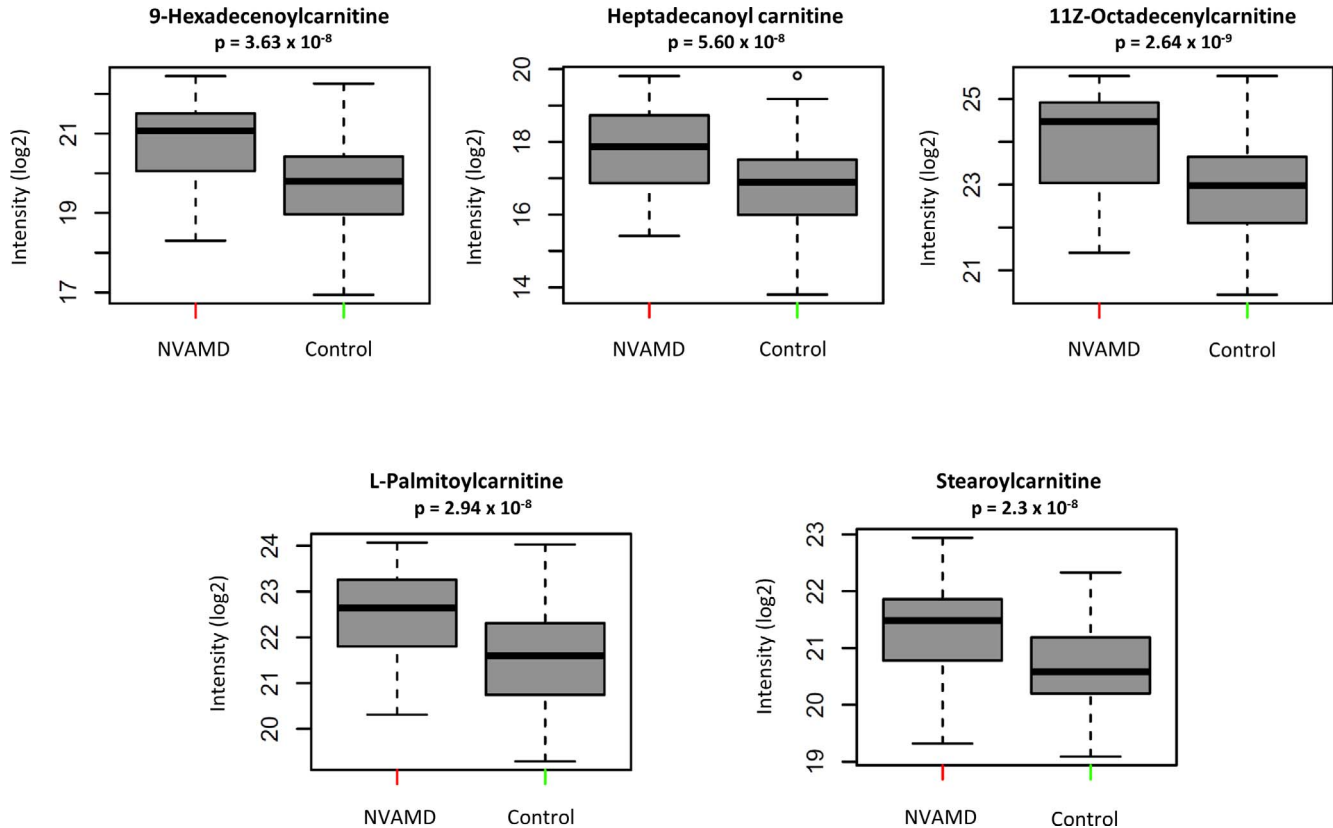

FIGURE 1. Plasma levels of multiple long-chain acylcarnitines are increased in NVAMD patients. Five long-chain acylcarnitines identified in the training set via untargeted metabolomics and confirmed with LC-MS/MS are significantly increased in NVAMD patients (*n* = 70) compared to controls (*n* = 134).
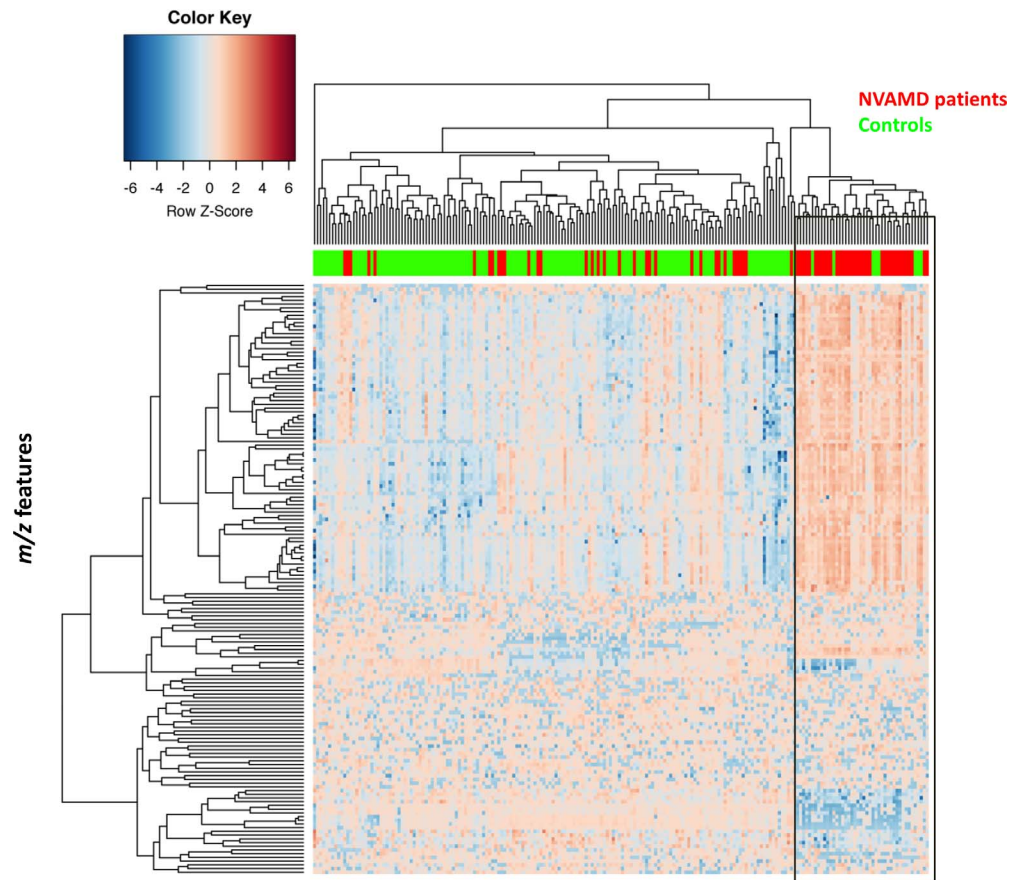
Figure 2. Two-way hierarchical cluster analysis of the 159 discriminating features and NVAMD patients and non-AMD controls. Each column represents an individual patient's metabolic profile based on the 159 features identified by nested feature selection. The cluster analysis includes only those NVAMD patients (*red*) and controls (*green*) from the training set. Cluster 1 is indicated by the *black box*.

acylcarnitine levels observed here are specifically related to NVAMD or to AMD in general. Determining the timing of the increased acylcarnitine levels in relation to AMD development and progression could facilitate identification of potential therapeutic targets for AMD. Additionally, this study revealed heterogeneity in the metabolic profiles of clinically indistinguishable NVAMD patients. Determining the significance of these metabolic similarities and differences could lead to a greater understanding of disease progression and therapeutic response in AMD patients.

Acknowledgments

Disclosure: **S.L. Mitchell**, None; **K. Uppal**, None; **S.M. Williamson**, None; **K. Liu**, None; **L.G. Burgess**, None; **V. Tran**, None; **A.C. Umfress**, None; **K.L. Jarrell**, None; **J.N. Cooke Bailey**, None; **A. Agarwal**, None; **M. Pericak-Vance**, None; **J.L. Haines**, None; **W.K. Scott**, None; **D.P. Jones**, None; **M.A. Brantley Jr**, None

References

1. Wong WL, Su X, Li X, et al. Global prevalence of age-related macular degeneration and disease burden projection for 2020 and 2040: a systematic review and meta-analysis. *Lancet Glob Health*. 2014;2:e106–e116.

2. Bressler NM. Early detection and treatment of neovascular age-related macular degeneration. *J Am Board Fam Pract*. 2002;15:142–152.

3. Rudnicka AR, Kapetanakis VV, Jarrar Z, et al. Incidence of late-stage age-related macular degeneration in american whites: systematic review and meta-analysis. *Am J Ophthalmol*. 2015; 160:85–93.e3.

4. Fritsche LG, Igl W, Bailey JNC, et al. A large genome-wide association study of age-related macular degeneration highlights contributions of rare and common variants. *Nat Genet*. 2016;48:134–143.

5. Sobrin L, Seddon JM. Nature and nurture-genes and environment-predict onset and progression of macular degeneration. *Prog Retin Eye Res*. 2014;40:1–15.

6. Seddon JM, Reynolds R, Yu Y, Daly MJ, Rosner B. Risk models for progression to advanced age-related macular degeneration using demographic, environmental, genetic, and ocular factors. *Ophthalmology*. 2011;118:2203–2211.

7. Tan SZ, Begley P, Mullard G, Hollywood KA, Bishop PN. Introduction to metabolomics and its applications in ophthalmology. *Eye Lond Engl*. 2016;30:773–783.

8. Osborn MP, Park Y, Parks MB, et al. Metabolome-wide association study of neovascular age-related macular degeneration. *PLoS One*. 2013;8:e72737.

9. Laíns I, Duarte D, Barros AS, et al. Human plasma metabolomics in age-related macular degeneration (AMD) using nuclear magnetic resonance spectroscopy. *PLoS One*. 2017; 12:e0177749.

10. Laíns I, Kelly RS, Miller JB, et al. Human plasma metabolomics study across all stages of age-related macular degeneration identifies potential lipid biomarkers. *Ophthalmology*. 2017; 125:245–254.

11. Luo D, Deng T, Yuan W, Deng H, Jin M. Plasma metabolomic study in Chinese patients with wet age-related macular degeneration. *BMC Ophthalmol*. 2017;17:165.

12. Seddon JM, Sharma S, Adelman RA. Evaluation of the clinical age-related maculopathy staging system. *Ophthalmology*. 2006;113:260–266.

13. Age-Related Eye Disease Study Research Group. The Age-Related Eye Disease Study (AREDS): design implications. AREDS report no. 1. *Control Clin Trials*. 1999;20:573–600.

14. Go Y-M, Walker DI, Liang Y, et al. Reference standardization for mass spectrometry and high-resolution metabolomics applications to exposome research. *Toxicol Sci Off J Soc Toxicol*. 2015;148:531–543.

15. Johnson JM, Yu T, Strobel FH, Jones DP. A practical approach to detect unique metabolic patterns for personalized medicine. *Analyst*. 2010;135:2864–2870.

16. Osborn MP, Park Y, Parks MB, et al. Metabolome-wide association study of neovascular age-related macular degeneration. *PLoS One*. 2013;8:e72737.

17. Soltow QA, Strobel FH, Mansfield KG, Wachtman L, Park Y, Jones DP. High-performance metabolic profiling with dual chromatography-Fourier-transform mass spectrometry (DC-FTMS) for study of the exposome. *Metabolomics*. 2013; 9(suppl 1):S132–S143.

18. Frediani JK, Jones DP, Tukvadze N, et al. Plasma metabolomics in human pulmonary tuberculosis disease: a pilot study. *PLoS One*. 2014;9:e108854.

19. Burgess LG, Uppal K, Walker DI, et al. Metabolome-wide association study of primary open angle glaucoma. *Invest Ophthalmol Vis Sci*. 2015;56:5020–5028.

20. Roede JR, Uppal K, Park Y, et al. Serum metabolomics of slow vs. rapid motor progression Parkinson's disease: a pilot study. *PLoS One*. 2013;8:e77629.

21. Yu T, Park Y, Johnson JM, Jones DP. apLCMS–adaptive processing of high-resolution LC/MS data. *Bioinforma Oxf Engl*. 2009;25:1930–1936.

22. Uppal K, Soltow QA, Strobel FH, et al. xMSanalyzer: automated pipeline for improved feature detection and downstream analysis of large-scale, non-targeted metabolomics data. *BMC Bioinformatics*. 2013;14:15.

23. Johnson WE, Li C, Rabinovic A. Adjusting batch effects in microarray expression data using empirical Bayes methods. *Biostat Oxf Engl*. 2007;8:118–127.

24. Patel RM, Roback JD, Uppal K, Yu T, Jones DP, Josephson CD. Metabolomics profile comparisons of irradiated and nonirradiated stored donor red blood cells. *Transfusion (Paris)*. 2015;55:544–552.

25. Gevaert O, De Smet F, Timmerman D, Moreau Y, De Moor B. Predicting the prognosis of breast cancer by integrating clinical and microarray data with Bayesian networks. *Bioinforma Oxf Engl*. 2006;22:e184–190.

26. Slawski M, Daumer M, Boulesteix A-L. CMA: a comprehensive bioconductor package for supervised classification with high dimensional data. *BMC Bioinformatics*. 2008;9:439.

27. He Z, Yu W. Stable feature selection for biomarker discovery. *Comput Biol Chem*. 2010;34:215–225.

28. Uppal K, Walker DI, Jones DP. xMSannotator: an R package for network-based annotation of high-resolution metabolomics data. *Anal Chem*. 2017;89:1063–1067.

29. Li S, Park Y, Duraisingham S, et al. Predicting network activity from high throughput metabolomics. *PLoS Comput Biol*. 2013;9:e1003123.

30. Li S, Sullivan NL, Rouphael N, et al. Metabolic phenotypes of response to vaccination in humans. *Cell*. 2017;169:862–877.e17.

31. Smith CA, Want EJ, O'Maille G, Abagyan R, Siuzdak G. XCMS: processing mass spectrometry data for metabolite profiling using nonlinear peak alignment, matching, and identification. *Anal Chem*. 2006;78:779–787.

32. Tautenhahn R, Böttcher C, Neumann S. Highly sensitive feature detection for high resolution LC/MS. *BMC Bioinformatics*. 2008;9:504.

33. Benton HP, Want EJ, Ebbels TMD. Correction of mass calibration gaps in liquid chromatography-mass spectrometry metabolomics data. *Bioinforma Oxf Engl*. 2010;26:2488–2489.

34. Ruttkies C, Schymanski EL, Wolf S, Hollender J, Neumann S. MetFrag relaunched: incorporating strategies beyond in silico fragmentation. *J Cheminformatics*. 2016;8:3.

35. Rist MJ, Roth A, Frommherz L, et al. Metabolite patterns predicting sex and age in participants of the Karlsruhe Metabolomics and Nutrition (KarMeN) study. *PLoS One*. 2017;12:e0183228.

36. Pennington KL, DeAngelis MM. Epidemiology of age-related macular degeneration (AMD: associations with cardiovascular disease phenotypes and lipid factors. *Eye Vis*. 2016;3:34.

37. Sharma S, Black SM. Carnitine homeostasis, mitochondrial function, and cardiovascular disease. *Drug Discov Today Dis Mech*. 2009;6:e31–e39.

38. Sardell RJ, Bailey JNC, Courtenay MD, et al. Whole exome sequencing of extreme age-related macular degeneration phenotypes. *Mol Vis*. 2016;22:1062–1076.

39. Guasch-Ferré M, Zheng Y, Ruiz-Canela M, et al. Plasma acylcarnitines and risk of cardiovascular disease: effect of Mediterranean diet interventions. *Am J Clin Nutr*. 2016;103: 1408–1416.

40. Ruiz M, Labarthe F, Fortier A, et al. Circulating acylcarnitine profile in human heart failure: a surrogate of fatty acid metabolic dysregulation in mitochondria and beyond. *Am J Physiol Heart Circ Physiol*. 2017;313:H768–H781.

41. Sun L, Liang L, Gao X, et al. Early prediction of developing type 2 diabetes by plasma acylcarnitines: a population-based study. *Diabetes Care*. 2016;39:1563–1570.

42. Sumner LW, Amberg A, Barrett D, et al. Proposed minimum reporting standards for chemical analysis Chemical Analysis Working Group (CAWG) Metabolomics Standards Initiative (MSI). *Metabolomics Off J Metabolomic Soc*. 2007;3:211–221.

43. Schymanski EL, Jeon J, Gulde R, et al. Identifying small molecules via high resolution mass spectrometry: communicating confidence. *Environ Sci Technol*. 2014;48:2097–2098.